

MANUFACTURING AND MACROSCOPIC PROPERTIES OF Y_2O_3 COATING LAYER ON CERAMIC (AlN) SUBSTRATE FABRICATED BY AEROSOL DEPOSITION

This study attempted to manufacture an Y_2O_3 ceramic coating layer on a ceramic (AlN) substrate using aerosol deposition (AD) and investigated its macroscopic properties. Pure Y_2O_3 powder with a polygonal shape and average size of $5.0 \mu m$ was used as initial feedstock. Using aerosol deposition with suitable process conditions, an Y_2O_3 coating layer was successfully fabricated on aluminum nitride (AlN). The thickness of the manufactured coating layer was approximately 10 nm. The coating layer consisted of Y_2O_3 phase identical to that in the initial powder, and no additional oxides were identified. In regard to the roughness of the Y_2O_3 coating layer, the average roughness (R_a) measured $1.32 \mu m$, indicating that the surface roughness was relatively even compared to the initial powder size ($5 \mu m$). Mechanical properties of the Y_2O_3 coating layer were measured using nano indentation equipment, and the indentation modulus of the Y_2O_3 coating layer fabricated by aerosol deposition measured 136.5 GPa. The interface of the coating layer was observed using TEM, and the deposition mechanism of the Y_2O_3 coating layer manufactured by aerosol deposition was also discussed.

Keywords: Aerosol deposition, Y_2O_3 coating layer, AlN matrix, Nano indentation

1. Introduction

Aluminum nitride (AlN) consists of a wurtzite crystal structure with a strong covalent bond. AlN features high heat conductivity and insulation, as well as high corrosion resistance against fluoride and chloride. Such properties allow AlN to be used as component material for high-temperature substrate, the material for the dry etching and CVD processes of semiconductor production [1]. In the case of the etching process for semiconductor production, technological advancements have been made to respond to the increase in wafer size and microfabrication technology of semiconductor devices. Accordingly, a dry etching process using a halogen gas plasma rather than a wet etching process has been used in recent years. As plasma is used for the process, many semiconductor process components are exposed to high-temperature corrosion environments. AlN, quartz and Al_2O_3 have conventionally been used as component materials, but the need for alternative with greater plasma resistance property is increasing. Yttria (Y_2O_3) is attracting more attention as a new alternative.

Yttria is known to feature greater plasma resistance compared to conventional materials (AlN, quartz, and Al_2O_3 , etc.) [2]. However, the cost of yttria is high and it is difficult to undergo sintering, which results in difficulty in manufacturing bulk products. Therefore, yttria is mainly used for coating processes.

Conventionally, plasma spraying was mainly used for yttria coating, and chemical vapor deposition (CVD) and physical vapor deposition (PVD) coating methods were reported to be used [3,4]. However, the plasma spraying, easily forms cracks due to the thermal expansion coefficient difference with the substrate and is limited in forming high-density coating layers. Physical and chemical deposition methods (PVD, CVD) are suited for depositing high-density coating layers, but it is very difficult to form thick coating layers and requires significant cost and time. In order to resolve such issues, new manufacturing technology for yttria (Y_2O_3) coating layer is demanded.

Unlike plasma spraying, which uses high energy sources, aerosol deposition coating process is performed at room temperature, therefore it does not cause the formation of oxides and phase transformation of powder [5]. Furthermore, the method causes plastic deformation and fragmentation as it collides ceramic powders of nano- to sub-micro size into the substrate with high kinetic energy. As a result, a highly dense coating layer can be obtained. At present, most studies of manufacturing coating layers by aerosol deposition feature depositing of ceramic particles on metal substrates, and there is no study that attempted to deposit a ceramic coating layer on a ceramic substrate such as AlN.

This study attempted to manufacture an Y_2O_3 coating layer on a ceramic substrate (AlN) by aerosol deposition, and then it investigated the microstructure and mechanical properties of the

* INHA UNIVERSITY, DEPT. MATERIALS SCIENCE & ENGINEERING, INCHEON 22212, REPUBLIC OF KOREA

** KSD KOREA, ANDONG 36729, REPUBLIC OF KOREA

Corresponding author: keeahn@inha.ac.kr

coating layer manufactured. In addition, this study also discussed the micro deposition mechanism of the aerosol-deposited Y_2O_3 coating layer.

2. Experimental

Fig. 1 shows the microstructural analysis (particle size, phase analysis) of the powder feedstock used for aerosol deposition in this study. The powder had a polygonal shape, particle size distribution of 1.88~12.06 μm and average particle size of approximately 5 μm .

TABLE 1

Aerosol deposition process conditions used in this study

Consumption of carrier gas	7 L/min.
Carrier gas	N_2
Standoff distance	5 mm
Pass number	5
Gun traverse speed	1 mm/s
Chamber pressure	2.4×10^{-1} torr

Table 1 lists the aerosol deposition conditions used in this study. The carrier gas used was N_2 and the chamber pressure was set and maintained at 2.4×10^{-1} torr. Nozzle distance was set at 5mm, and the Y_2O_3 coating layer was manufactured at a transfer speed of 1mm/s. To observe the microstructure of the Y_2O_3 coating layer and substrate, the specimen was polished with SiC paper (#400~2000) and alumina (Al_2O_3) slurry, and then was finished with colloidal silica. For microstructural analysis, a field emission scanning electron microscope (FE-SEM) (Tescan, MYRA-3XMH) and transmission electron microscope (TEM) (JEM-2010) were used. For phase analysis and roughness measurement, an X-ray diffractometer (XRD) (Ultima IV) and a 3D profiler (Contour GT-X) were used. To evaluate the mechanical properties of the coating layer, nano indentation (Helmut Fisher Co., HM 500) equipment was used to implement tests with a load of 40 mN and loading time of 15 sec.

3. Results and discussion

Fig. 2a is a macro image of the Y_2O_3 coating layer manufactured by aerosol deposition. It was confirmed that the Y_2O_3 coat-

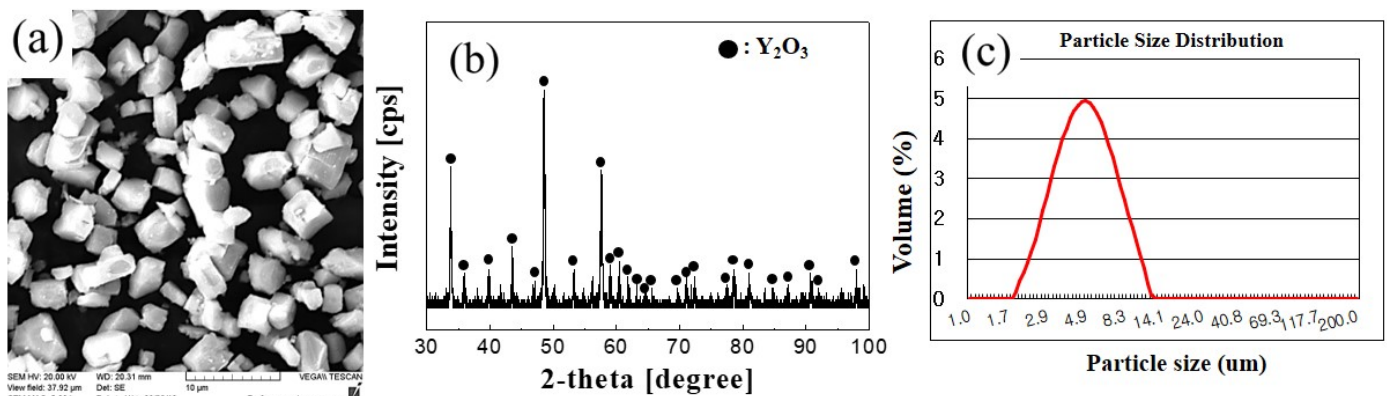


Fig. 1. Y_2O_3 powder feedstock analysis results: (a) powder shapes, (b) XRD analysis and (c) particle size distribution

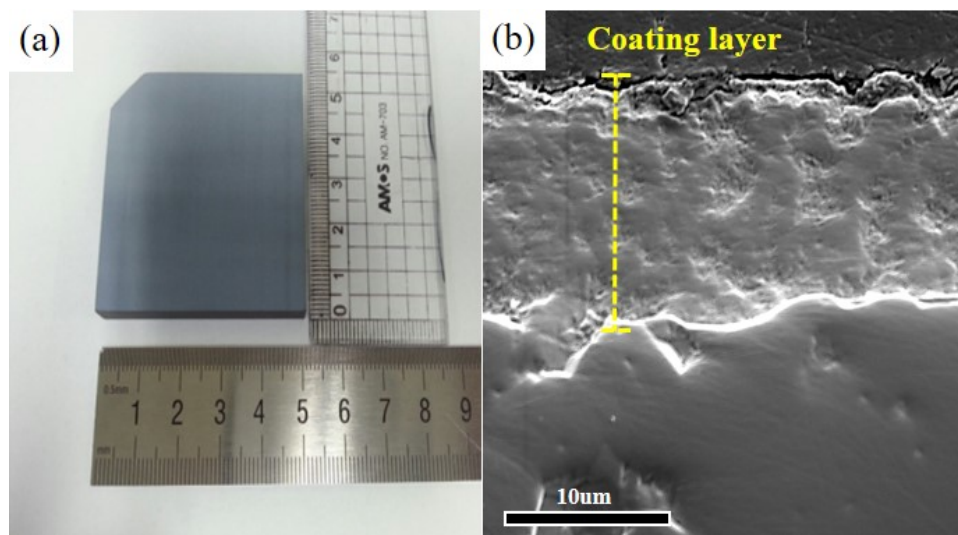


Fig. 2. (a) Macro observation and (b) cross-section observation results of Y_2O_3/AlN manufactured by aerosol deposition

ing material was evenly deposited on an area of 27.5 cm² (length 50 mm, width 55 mm), and no massive cracks were observed in the coating layer. In addition, no spalling of the coating layer from the AlN substrate occurred. Fig. 2b is the cross-sectional observation of the manufactured coating material. The coating material measured approximately 10 μm in thickness, and no cracks were observed at the interface between the AlN substrate and Y₂O₃ coating layer. The manufactured coating layer featured a dense structure with nearly no pores.

Fig. 3 is the XRD phase analysis results of the AlN substrate and Y₂O₃ coating layer. The substrate was composed of AlN phase. In the case of the manufactured Y₂O₃ coating layer, AlN peaks were detected due to the layer's thin thickness. The Y₂O₃ coating layer did not undergo any phase transformation and featured pure Y₂O₃ phase identical to that of the initial powder (Fig. 1). This result shows the evidence of the advantage of the room temperature depositing process.

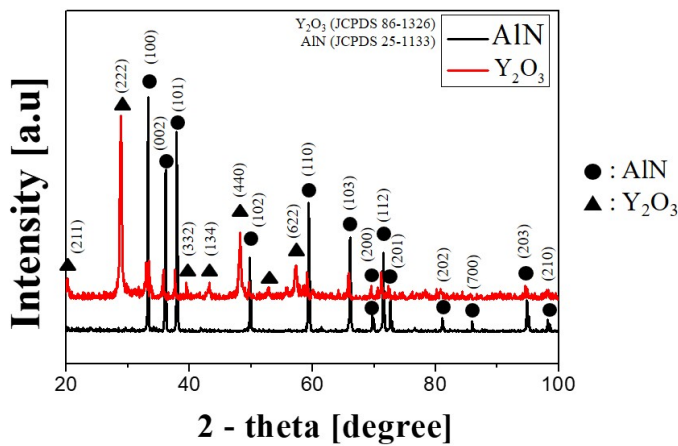


Fig. 3. XRD analysis results of AlN substrate and Y₂O₃ coating layer

To measure the roughness of the fabricated coating layer, 3D profiler analysis was performed, and its results are shown in Fig. 4. The surface roughness of the coating layer, R_a value (average roughness) measured 1.32 μm. Considering the size of the initial powder (average ~5 μm), the surface roughness is

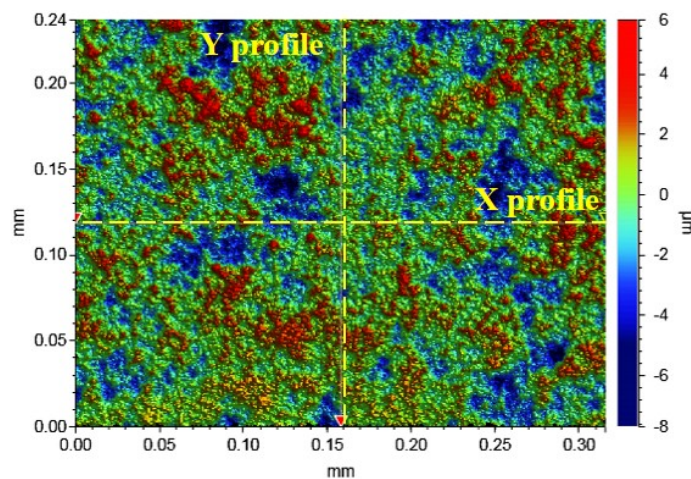


Fig. 4. Surface roughness analysis results of Y₂O₃ coating layer

relatively even. It can be understood that the even surface was formed due to powder particles accelerated by aerosol deposition having sufficient kinetic energy to the particles to be fractured by collision with the substrate and coating layer.

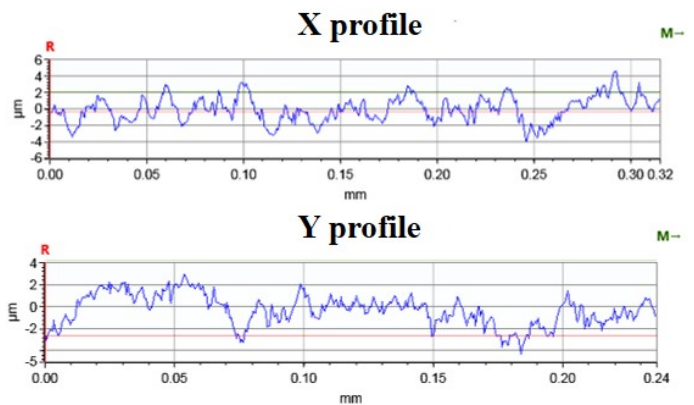
Fig. 5a,b are the SEM and TEM observation results of the interface area of Y₂O₃ coating layer and AlN substrate. TEM analysis did not identify features of the initial powder (polygonal shape of 5 μm) at the coating layer and interface. The Y₂O₃ powder, with an average size of 5 μm, was confirmed to be fractured into particles ranging from 10 s to 100 s of nm due to the high kinetic energy and deposited on the substrate (Fig. 5c). From the interface between the coating layer and substrate, anchoring areas, which cause plastic deformation of the substrate due to the collision of particles and the substrate, were observed (Fig. 5a,b). V. Audurier [6] reported that AlN achieves an elongation of 6.5% in a compression test at room temperature. Based on such, this study suspects that the high pressure formed during particle collision was absorbed by the AlN through deformation, resulting in the formation of an anchoring layer. In the case of the Y₂O₃ coating layer, it was confirmed that Y₂O₃ was additionally deposited due to room temperature impact consolidation (RTIC) caused by particle fracturing and continuous hammering effect on the initial deposited Y₂O₃ layer [7].

TABLE 2

Indentation results of Y₂O₃ coating layer manufactured by aerosol deposition

Properties	H _{IT}	E _{IT}	H _v
Y ₂ O ₃ coating layer	4.05 GPa	136.5 GPa	383.4 H _v

Table 2 lists the results of the nano indentation test implemented to evaluate the mechanical properties of the manufactured coating layer. The manufactured coating layer measured H_{IT} (indentation hardness): 4.05 GPa, E_{IT} (indentation modulus): 136.5 GPa and H_v: 383.4 H_v. The results above are slightly less than the indentation hardness of sintered Y₂O₃ [8]. This is suspected to be due to the nano-sized pores present within the coating layer. E. S. Park et al. [9] manufactured



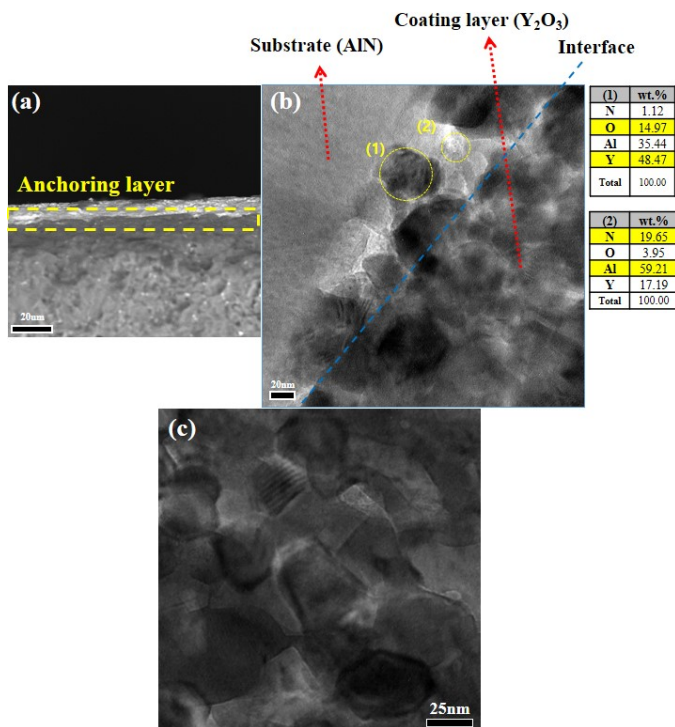


Fig. 5. (a) SEM image, (b) TEM image of Y_2O_3/AlN interface, and (c) TEM image of Y_2O_3 coating layer interior

a metal (Sn, Al and SUS 316 alloy) substrate and Y_2O_3 coating layer on an amorphous substrate using aerosol deposition. The manufactured Y_2O_3 coating layer was reported to achieve hardness (H_v) of Sn substrate: 86 Hv, Al substrate: 196 Hv, SUS316 substrate: 418 Hv and Amorphous substrate: 447 Hv [9]. In other words, the hardness (H_v) of the deposited Y_2O_3 coating layer on a ceramic substrate this study manufactured has greater or slightly lower hardness than the Y_2O_3 coating layer on a metal substrate and slightly lower hardness than a coating layer on an amorphous substrate.

The aerosol-deposited Y_2O_3 coating material this study was able to be manufactured on a large area of 27.5 cm^2 evenly and quickly, and it featured physical properties similar to Y_2O_3 coating layers on metal substrates. Based on such findings, the possibility of applying aerosol deposition to manufacture components requiring Y_2O_3 on ceramic substrate in the semiconductor industry, as well as various other industries, was confirmed.

4. Conclusions

This study manufactured an Y_2O_3 coating layer on an AlN ceramic substrate using aerosol deposition, and microstructural observation and an indentation test were implemented on the material. No macro spalling or defects were observed in the manufactured Y_2O_3 coating layer. The coating layer was composed of pure Y_2O_3 phase that was identical to the powder feedstock, and no additional impurities were formed. TEM observation confirmed that the initial $5\text{ }\mu\text{m}$ powder particles fractured into 10s of nano-sized particles as they collided with the substrate, and anchoring areas were formed at the interface. The coating layer is suspected to be deposited by room temperature impact consolidation due to particle fracturing and a hammering effect. The indentation test confirmed that the manufactured Y_2O_3 coating layer achieved H_{IT} (indentation hardness): 4.05 GPa, E_{IT} (indentation modulus): 136.5 GPa and H_v : 383.4 H_v .

Acknowledgments

This research was technically supported by Helmut Fisher Co.

REFERENCES

- [1] S.G. Ko, CERAMIST **14**, 29 (2011).
- [2] C.S. Kim, M.J. Kim, H. Cho, T.E. Park, Y.H. Yun, Ceram. Int. **41**, 12757 (2015).
- [3] Y.C. Cao, L. Zhao, J. Luo, K. Wang, B.P. Zhang, H. Yokota, Y. Ito, J.F. Li, Appl. Surf. Sci. **366**, 304 (2016).
- [4] D.M. Kim, S.Y. Yoon, K.B. Kim, H.S. Kim, Y.S. Oh, S.M. Lee, J. Korean Ceram. Soc., **45**, 707 (2008).
- [5] G.S. Ham, S.H. Kim, J.Y. Park, K.A. Lee, Arch. Metall. Mater. **62**, 1347 (2017).
- [6] V. Audurier, J.L. Demenet, J. Rabier, Philo. Mag. A **77**, 825 (1998).
- [7] J. Akedo, J. Therm. Spray Technol. **17**, 181 (2008).
- [8] B. Ahmadi, S.R. Reza, M.A. Vadeqani, M. Barekat, Ceram. Int. **42**, 17081 (2016).
- [9] J. Kim, J.I. Lee, D.S. Park, E.S. Park, J. Appl. Phys. **117**, 014903 (2015).